Activation of Platelet-Activating Factor Receptor and Pleiotropic Effects on Tyrosine Phospho-EGFR/Src/FAK/Paxillin in Ovarian Cancer

Margarita Aponte,[1] Wei Jiang,[1] Montaha Lakkis,[2] Ming-Jiang Li,[1] Dale Edwards,[1] Lina Albitar,[1] Allison Vitonis,[1] Samuel C. Mok,[1] Daniel W. Cramer,[1] and Bin Ye[1]

[1]Laboratory of Gynecologic Oncology and Epidemiology, Department of Obstetrics and Gynecology and Reproductive Biology, Brigham and Women's Hospital, Dana-Farber Cancer Center, Harvard Medical School, Boston, Massachusetts and [2]BioSource, Invitrogen, Inc., Carlsbad, California

Abstract

Among the proinflammatory mediators, platelet-activating factor (PAF, 1-*O*-alkyl-2-acetyl-*sn*-glycero-3-phosphorylcholine) is a major primary and secondary messenger involved in intracellular and extracellular communication. Evidence suggests that PAF plays a significant role in oncogenic transformation, tumor growth, angiogenesis, and metastasis. However, PAF, with its receptor (PAFR) and their downstream signaling targets, has not been thoroughly studied in cancer. Here, we characterized the PAFR expression pattern in 4 normal human ovarian surface epithelial (HOSE) cell lines, 13 ovarian cancer cell lines, paraffin blocks (n = 84), and tissue microarrays (n = 230) from patients with ovarian cancer. Overexpression of PAFR was found in most nonmucinous types of ovarian cancer but not in HOSE and mucinous cancer cells. Correspondingly, PAF significantly induced cell proliferation and invasion only in PAFR-positive cells (i.e., OVCA429 and OVCA432), but not in PAFR-negative ovarian cells (HOSE and mucinous RMUG-L). The dependency of cell proliferation and invasion on PAFR was further confirmed using PAFR-specific small interfering RNA gene silencing probes, antibodies against PAFR and PAFR antagonist, ginkgolide B. Using quantitative multiplex phospho-antibody array technology, we found that tyrosine phosphorylation of EGFR/Src/FAK/paxilin was coordinately activated by PAF treatment, which was correlated with the activation of phosphatidylinositol 3-kinase and cyclin D1 as markers for cell proliferation, as well as matrix metalloproteinase 2 and 9 for invasion. Specific tyrosine Src inhibitor (PP2) reversibly blocked PAF-activated cancer cell proliferation and invasion. We suggest that PAFR is an essential upstream target of Src and other signal pathways to control the PAF-mediated cancer progression. [Cancer Res 2008;68(14):5839–48]

Introduction

Platelet-activating factor (PAF), prostaglandins, and lysophosphatidic acid are three major phospholipid mediators shown to be involved in many different biological pathways in inflammatory diseases and cancer (1–5). Molecular pathways regulated by prostaglandins and lysophosphatidic acid have been extensively studied in many cancers (6–9), including ovarian cancer (10). Their importance is underscored by the emergence of COX inhibitors and nonsteroidal anti-inflammatory drugs as potent anticancer agents targeting prostaglandins and lysophosphatidic acid (11). Like prostaglandins and lysophosphatidic acid, PAF is an important proinflammatory activator of platelets, neutrophils, macrophages, lymphocytes, and endothelial cells, which are often essential microenvironmental components interacting with cancer cells (12–14).

PAF induces its multiple cellular effects through its specific receptor, PAFR, which belongs to the G protein–coupled receptor family and transduces cell signals via the G proteins and associated protein phosphorylation cascades (15, 16). PAF also plays a significant role in oncogenic transformation (17), antiapoptosis (18), metastasis (19), and angiogenesis in several types of cancers (20). Transgenic mice overexpressing PAFR displayed proliferative disorders and melanocytic tumors (21). In normal rat fibroblasts overexpressing PAFR, PAF induced immediate early oncogene expression and mitogenic responses (17). In addition, many types of cells, when challenged with PAF, displayed activation of tyrosine kinase (22) and protein phosphorylation (23). PAF induces early tyrosine phosphorylation signals through focal adhesion kinase (FAK) and paxillin in human endothelial cells (24), and induces cell proliferation through EGFR activation in keratinocytes (25). However, the significance of these tyrosine phosphorylation signaling pathways associated with PAF-PAFR has not been characterized in human cancers including ovarian cancer, the most lethal gynecologic malignancy associated with abnormal lipid and hormonal metabolism (26, 27).

Ginkgolide B, a specific antagonist of PAFR, is found exclusively in the herbal Ginkgo biloba. Our previous studies showed that ginkgolide B specifically inhibits nonmucinous ovarian cancer proliferation via cell cycle blockage (28). This suggests that different subtypes of ovarian cancer cells might have different PAFR expression profiles that mediate the ginkgolide B response. We hypothesize that ovarian cancer cell lines and tissue specimens with different PAFR gene expressions would be a valuable model system to investigate the regulatory mechanisms of PAF-PAFR with its associated signal pathways in ovarian cancer progression.

In this study, we have characterized the *PAFR* gene and protein expression in different subtypes of ovarian cancer cell lines and tissue specimens collected from different histologic subtypes of ovarian cancers. Potential PAFR-dependent biological functions, including cell proliferation and invasion, were examined by blockage using PAFR-specific antibody, antagonist ginkgolide B,

Note: M. Aponte and W. Jiang have contributed equally to this article.

Current address for W. Jiang: Obstetrics and Gynecology Hospital of Fudan University, 419 Fang Xie Road, Shanghai 200011, P.R. China. Current address for M. Aponte: Obstetrics and Gynecology, Northwestern University, Chicago, IL.

Requests for reprints: Bin Ye, Harvard Medical School, 221 Longwood Avenue, LMRC 610, Boston, MA 02115. Phone: 617-732-6976; Fax: 617-264-5248; E-mail: bye@partners.org.

doi:10.1158/0008-5472.CAN-07-5771

and small interfering RNA (siRNA) gene silencing probes. Using the phospho-antibody microarray technology, phosphorylation of a set of oncoprotein targets (EGFR/Src/FAK/paxillin) induced by PAF was evaluated in OVCA429 ovarian cancer cells and further validated in OVCA432 and RMUG-L cells with positive and negative PAFR expression, respectively.

Materials and Methods

Chemical reagents. DMSO, PAF, and ginkgolide B (>90% high-performance liquid chromatography grade), cell culture mediums of MCDB-105 and medium 199 were purchased from Sigma-Aldrich and F12 from Invitrogen. Mercator Array phospho-8-Plex and the relevant phospho-antibodies were purchased from BioSource, Invitrogen. Kinase inhibitor PP2 was purchased from Sigma-Aldrich, A25 and LY294002 were from Calbiochem, and erlotinib was from LC Laboratories.

Tissue samples. Paraffin-embedded tissue was assembled from specimens collected and archived from patients who had undergone primary surgery at Brigham and Women's Hospital (Boston, MA). All patient-derived specimens were collected under protocol approved by the Institutional Review Board at Brigham and Women's Hospital. Clinical stage and histologic subtype were defined by the International Federation of Gynecology and Obstetrics system.

Cell lines. Ovarian cancer cell lines derived from serous (DOV13, OVCA3, OVCA429, OVCA432, OVCA433, and SKOV3), mucinous (MCAS, RMUG-L, and RMUG-S), clear cell (ES2, TOV21G, and RMG1), and endometrioid (TOV112D) adenocarcinomas were used in this study. Cell lines SKOV3, RMG1, ES2, OVCAR3, MCAS, RMUG-L, RMUG-S, and TOV112D were purchased from American Type Culture Collection and Japanese Collection of Research Bioresources. Other cell lines were established in the Laboratory of Gynecologic Oncology at Brigham and Women's Hospital. Normal human ovarian surface epithelium (HOSE) cells were obtained from fresh ovarian scrapings at the time of surgery for benign conditions. Immortalized HOSE cells were obtained by transfection of primary HOSE cells with a retroviral vector expressing HPV-E6E7 oncogenes (29).

Cell culture and treatment. Cells were cultured in sterile 75 cm^2 cell culture flasks in MCDB 105 and medium 199 supplemented with 10% fetal bovine serum (Gemini Bioproducts) and 1% antibiotic (200 mmol/L L-glutamine, 10,000 units penicillin, and 10 mg/mL streptomycin). RMUG-S cells were cultured in F12 medium with 10% fetal bovine serum and 1% antibiotic as above. Cells were maintained at 37°C under 5% CO_2/95% air in a high-humidity chamber. Monolayer cells at 60% to 80% confluence were enzymatically removed using trypsin/EDTA and plated in 96-well flat-bottomed plates at a concentration of 1×10^3 per well for OVCA429 and OVCA432, 5×10^3 per well for HOSE-E6E7 cells and RMUG-L. After overnight plating and starving for 24 h in serum-free medium, cells were treated with different concentrations of PAF, ranging from 1 pmol/L to 1 μmol/L, tyrosine kinase inhibitor PP2 (10 μmol/L), A25 (10 μmol/L), and ginkgolide B (100 μmol/L). An equal volume of DMSO (<1% concentration) was used as a control. A polyclonal antibody against PAFR (1 μg/mL) was diluted in 1:2,000 to 1:50 in serum-free medium and calibrated with equal volume of nonspecific pure IgG as negative control.

Cell proliferation and invasion assay. Cell proliferation was assessed using a 3-(4,5-dimethylthiazol-2-yl)-2,5-diphenyltetrazolium bromide (MTT) assay (Promega; ref. 30). After 72 h of treatment, 10 μL of the MTT dye solution was added to each well and the plates were incubated at 37°C for 4 h in a humidified chamber. After incubation, 100 μL of the solubilization/stop solution was added to each well. One hour after the addition of the solubilization solution, the contents of the wells were mixed and read by the 96-well plate scanning spectrophotometer (μQuant) and quantitative software (KC-junior, Bio-Tek Instruments, Inc.) at an absorbance of 630 nm for quantitative analysis. Ginkgolide B, PAFR antibody, and inhibitors were pretreated with serum-free condition for 0.5 h in OVCA429 and OVCA432 cancer cells (10^4 per well coating) before the addition of PAF, followed by 72 h of treatment and MTT assay. Data was collected from at least two separate experiments and eight repeats were performed for each treatment. Cell proliferation activity was presented as a percentage of the control with an equivalent volume of DMSO (as 100%).

Cell invasion activity assay for OVCA429 and OVCA432 cells were done with an 8 μm Matrigel invasion chamber. Experiments were carried out according to the manufacturer's protocol. Briefly, each well insert was coated with 100 μL of a 1:10 mixture of Matrigel/serum-free medium, followed by incubation at 37°C for 4 h. After 0.5 h of pretreatment with inhibitor in serum-free condition, cells were then trypsin digested and transferred into top Matrigel wells (10^5 cancer cells per well) with the addition of 0.1% bovine serum albumin, inhibitor, and 100 nmol/L of PAF. Six hundred microliters of 10% fetal bovine serum medium was added to the bottom of the chamber and incubated at 37°C for 36 h. Ginkgolide B, PAFR antibody, and inhibitors (PP2 and A25) were pretreated with OVCA432 and OVCA429 cells for 1 h before the addition of PAF for 36 h in the invasion assay. Invasion activity was assessed by the number of cells that crossed the Matrigel and filter membrane. Filter membranes were fixed in 95% ethanol and stained with 0.1% crystal solution. Cell numbers were counted under a light microscope and presented as a percentage compared with the controls. Experiments were performed twice, with at least three repeats for each treatment.

RNA extraction and quantitative real-time PCR. Total RNA was isolated from 2 primary HOSE cell cultures, 2 immortalized HOSE cell lines, 13 ovarian cancer cell lines, and 84 ovarian cancer specimens including 8 mucinous, 9 serous high grade/early stage (Fig. 1*B*), 45 serous late stages invasive, 11 endometrioid, and 11 clear cell subtypes. The extraction of RNA was performed according to the manufacturer's protocol (Qiagen) and amplified using the Superscript First-Strand Synthesis System for reverse transcription-PCR (Invitrogen). Laser-captured microdissected tissue was processed for RNA extraction and cDNA amplification using the published method (31). RT-PCR primers (assay ID: HS00265399_s1) for PAFR and cyclophylin A, as the housekeeping gene, were purchased from Applied Biosystems. Each quantitative RT-PCR reaction started with a 10-min hold at 95°C, followed by 40 cycles of denaturation at 95°C for 125 s, followed by annealing/extending at 60°C for 1 min. All experiments were run in duplicate and repeated twice. The 7300 real-time PCR System software was used to monitor the amplification process and determine the threshold cycle (Ct) for each reaction. Quantification was performed using methods described previously (32).

Tissue microarray and immunohistochemistry. Five-micrometer sections of tissue microarrays were obtained from the Gynecologic Oncology Group tissue bank containing a tissue from 27 benign patients, 62 with mucinous, 30 with serous borderline, 43 with serous invasive, 28 with endometrioid, and 42 with clear cell tumors. Immunohistochemical analysis was carried out for PAFR protein expression. Human pancreatic tissue sections were used as a positive control. Immunohistochemistry was performed using the EnVision/AP system (DakoCytomation). This system used an anti-rabbit immunoglobulin conjugated to an alkaline phosphatase polymer (Labeled polymer-AP), which is revealed as a red stain after the addition of the Substrate-Chromogen solution. Slides were washed with deionized water and counterstained with hematoxylin and 5% ammonium hydroxide, and mounted in Accergel (Accurate Chemical and Scientific Corp.). The photomicrograph image was recorded by a digital camera (Optronic). Each subject had three independent readings by two investigators using a semiquantitative scoring system: 0, absent or trace staining; 1, minimal staining; 2, moderate staining; or 3, strong staining.

Western blot and antibodies. Cells were washed twice with 1× PBS and then lysed by protein lysis buffer containing phenylmethylsulfonyl fluoride and Protease Inhibitor Cocktail I and II (Sigma-Aldrich). After a brief vortexing and centrifuging at 4°C, the Bradford Protein Assay Kit (Bio-Rad) was used for protein quantification of the cell lysates. Total cell protein lysates were separated by 7% or 16% SDS-PAGE gel (10 μg per well) based on the size of protein detected. Proteins were transferred to polyvinylidene difluoride membrane (Perkin-Elmer) using the SEMI-DRY Transfer Cell (Bio-Rad Laboratories), and blocked with 5% fat-free dry milk at 4°C overnight. The membrane was subsequently washed and incubated with anti-PAFR antibody (Cayman Chemical) in blocking solution at 1:125 dilution for 2 h. Following three washes, secondary anti-rabbit IgG antibody

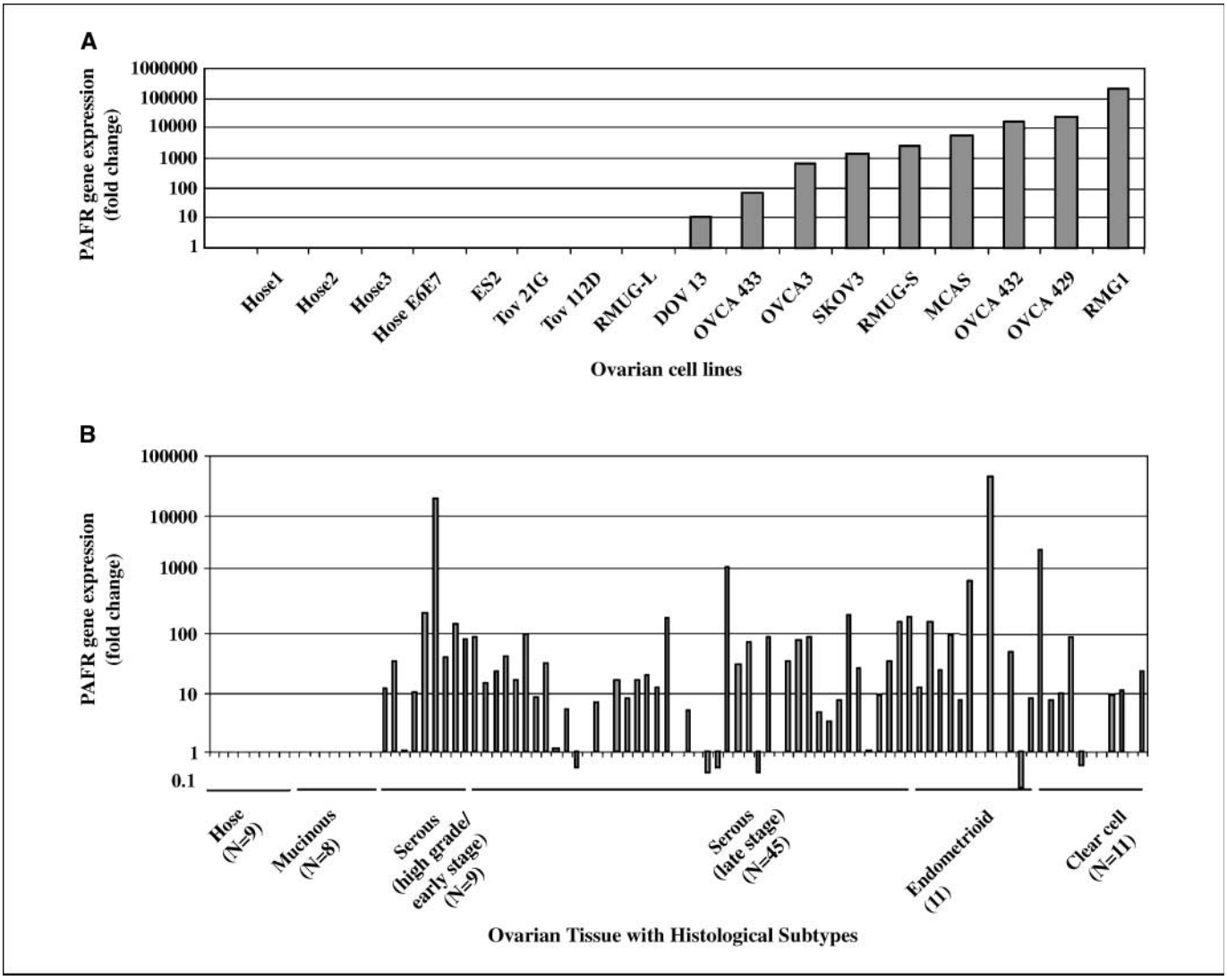

Figure 1. *PAFR* gene expression in ovarian cancer cell lines and ovarian cancer tissue specimens. Quantitative real-time PCR was performed using isolated total RNA extracts. Amplified cDNA was calibrated with the housekeeping gene cyclophylin A. Relative *PAFR* gene expression level in ovarian cancer cell lines was normalized with normal HOSE (*A*). The relative *PAFR* gene expression of ovarian cancer cells isolated from the LCM microdissected cancerous cells from the slides of individual cancer patients was present as fold-of-increase compared with the *PAFR* expression in the normal HOSE cells (*B*).

(1:2,000) with peroxidase conjugate was used to reveal the protein expression signals with chemiluminescent kit (Pierce Chemical, Co.). Similar approach was used to detect phospho-EGFR, FAK, paxillin, Src, and protein phosphatidylinositol 3-kinase (PI3K), cyclin D1, matrix metalloproteinase (MMP) 2 and MMP9 (Cell Signaling Technology), with 1:1,000 dilution for the primary antibodies.

SiRNA treatment. Three predesigned PAFR siRNA probes and a silencer negative control siRNA were purchased from Ambion. The PAFR siRNAs were targeted to exon 2 (P1 sense, GGGAUAUCUACUGUGGUCUtt; antisense AGACCACAGUAGAUAUCCCtt; P2 sense, CCCUGUUAUCUACUACUGUUUCtt; antisense, GAAACAGUAGAUAACAGGGtc; P3 sense, GGCCAUUAAUGAUGCACAUtt; antisense, AUGUGCAUCAUUAAUGGCCtg). Reverse transfection was carried out using siPORT amine (Ambion) with a final concentration of 30 nmol/L siRNA. After 24 h of incubation, the medium was replaced to decrease toxicity. Knockdown of PAFR gene expression was verified by quantitative RT-PCR and further confirmed by Western blot after 72 h of initial transfection. Specific silencing of targeted genes was confirmed by three independent experiments.

Phospho-array analysis. We analyzed the differential phosphorylation of multiple signaling phospho-proteins of EGFR (pY^{1068}), mitogen-activated protein kinase (MAPK) p38 ($pTpY^{180/182}$), Akt/PKB (pS^{473}), FAK (pY^{397}), Src (pY^{418}), paxillin (pY^{118}), HSP27 (pS^{82}), and ATF2 ($pTpT^{69/71}$) using Invitrogen Mercator Cell Adhesion 8-Plex phosphoarray. Briefly, 16 pad-slides were first blocked with 70 μL of polymer-based blocking buffer for 15 min prior to adding the protein samples, purified calibration standards or lysates prepared from OVCA429 cells of untreated control, treated with PAF alone (100 nmol/L), or PAF (100 nmol/L) and ginkgolide B (100 μmol/L) at different time points. Seventy microliters of each of the eight diluted samples was added to determine the standard curve for each of the 8-Plex markers. Additionally, control and treated lysates were also evaluated for the phosphorylation level of the 8-Plex markers, in which 70 μg of protein lysates were added per well and incubated with mild shaking for 3 h at room temperature. The unbound materials were subsequently removed from the wells by washing. Next, 125 μL (1 mg/mL) of the "array-detector-antibody" containing a mixture of all eight polyclonal phospho-antibodies was added to each pad and incubated for 1 h at room temperature. Following three washing steps with 90 μL of TBST, the wells were incubated with 70 μL (1 μg/mL) of the fluorescently conjugated secondary antibody for 45 min at room temperature. At the completion of incubation, the slides were washed thrice with 90 μL of TBST buffer and then quickly rinsed in

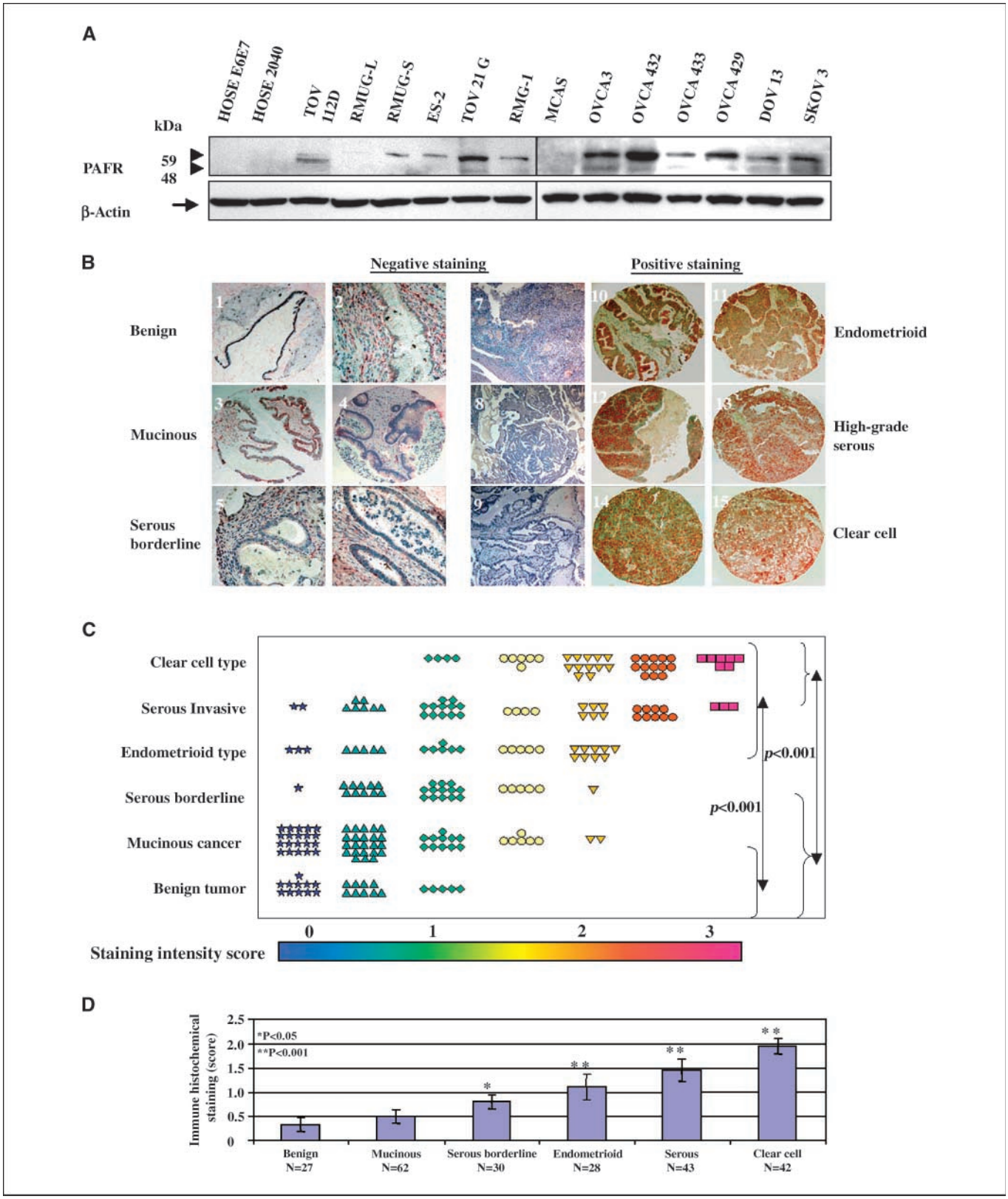

Figure 2. PAFR protein expression patterns in ovarian cancer cell lines and ovarian cancer tissue specimens. *A,* PAFR protein expression was revealed by Western blot with a specific polyclonal antibody against human PAFR. *B,* tissue microarray–based immunohistochemical staining with specific PAFR antibody showed that PAFR is negative or less detectable in benign, mucinous, and serous borderline tumors (*slides 1–6*), but overexpressed in clear cell type, endometrioid, and high-grade serous ovarian tumors (*slides 10–15*); negative control staining of the slides without primary antibody present (*slides 7–9*) for endometrioid, high-grade serous, and clear cell type, respectively. *C,* summary of the immune staining intensity scale (mean value of duplicates) for PAFR expression of the individual patient in different histologic subtypes. *D,* summary of immune staining intensity of PAFR expression in each subtype of patient groups. Significant difference between groups was statistically analyzed by using one-way ANOVA and Bonferroni multiple comparison tests (*, $P < 0.05$; **, $P < 0.001$).

distilled water. The slides were then allowed to dry for 5 min by incubating at 37°C. The phospho-array slides were scanned with an Axon Genepix scanner (Molecular Devices, Co.) for image acquisition and the data was analyzed using the ArrayVision software.

Statistical analysis. For the immune staining intensity and quantification, the average was derived from the individual intensity score for each subject and the mean value per subject was used to calculate the mean value for each group. ANOVA was used to test for differences in PAFR protein expression between case groups using a Bonferroni correction for multiple comparisons. A t test analysis was used to compare the protein expression level between early and late stage cases. ANOVA tests were used for analysis of the data derived from the cell proliferation and invasion assays to show the significance between treated and untreated cells in different experiments.

Results

PAFR gene expression pattern in ovarian cancer cell lines and tissue specimens. PAFR expression levels were significantly higher in 9 of the 13 cancer cell lines and exhibited up to 10,000-fold increase. PAFR gene expression was not detected in RMUG-L, TOV-21G, TOV112D, and ES2 cells when compared with the levels found in immortalized HOSE cells (Fig. 1*A*). To investigate the mRNA expression pattern in ovarian cancer tissue samples, total RNA was isolated from cultured ovarian cancer cell lines and the microdissected ovarian surface epithelial cancer cells from 84 patients with ovarian cancer. As shown in Fig. 1*B*, PAFR gene expression was undetectable in 9 HOSE cell lines and 8 mucinous samples. PAFR was overexpressed in ovarian cancer tissues but varied across different histologic subtypes of ovarian cancers. PAFR expression was significantly increased in 8 of 9 high-grade early stage serous (88.8%), 34 of 45 late stage serous invasive (75.5%), 8 of 11 endometrioid (72.7%), and 7 of 11 clear cell type cancers (63.6%) compared with normal ovarian cells and ranged from 10-fold to 10,000-fold greater.

We then examined PAFR protein expression by Western blot using the specific polyclonal antibody against human PAFR in a series of ovarian cancer cell lines. Immune blot analysis revealed that two specific PAFR protein bands at 48 kDa and 59 kDa were absent in the HOSE cell lines and two of three mucinous type cancer cells (RMUG-L, MCAS, and RMUG-S) and showed the upper positive band in endometrioid ovarian cancer cell line (TOV112D), three clear cell types (ES-2, TOV21G, RMG-1), and six serous type ovarian cancer cell lines (OVCA3, OVCA432, OVCA433, OVCA429, and DOV13 SKOV3; Fig. 2*A*). The molecular weight difference of PAFR proteins shown in Fig. 2*A* may be due to a splice variant of PAFR or posttranslational modification (33).

Immunohistochemical staining on the tissue microarrays containing different histologic types of preoperative tissue specimens revealed that PAFR protein expression was significantly higher in patients with ovarian cancer (n = 205) compared with that of benign ovarian tissue specimens (n = 35). There was a barely detectable staining in benign and mucinous cancers (Fig. 2*B*). PAFR expression was significantly (P < 0.001) higher in clear cell, serous invasive, and endometrioid types compared with mucinous and benign ovarian tumors. PAFR expression in nonmucinous malignant ovarian cancers was significantly (P < 0.001) higher when compared with the benign counterparts (Fig. 2*D*).

PAF-induced ovarian cancer cell proliferation is PAFR-dependant. To determine the biological function of PAFR on ovarian cancer cell growth, the PAFR-negative normal (HOSE-E6E7) cell line and mucinous cell line (RMUG-L), and two PAFR-positive serous type of ovarian cancer cell lines (OVCA429/OVCA432) were selected for the proliferation assay. PAF and a

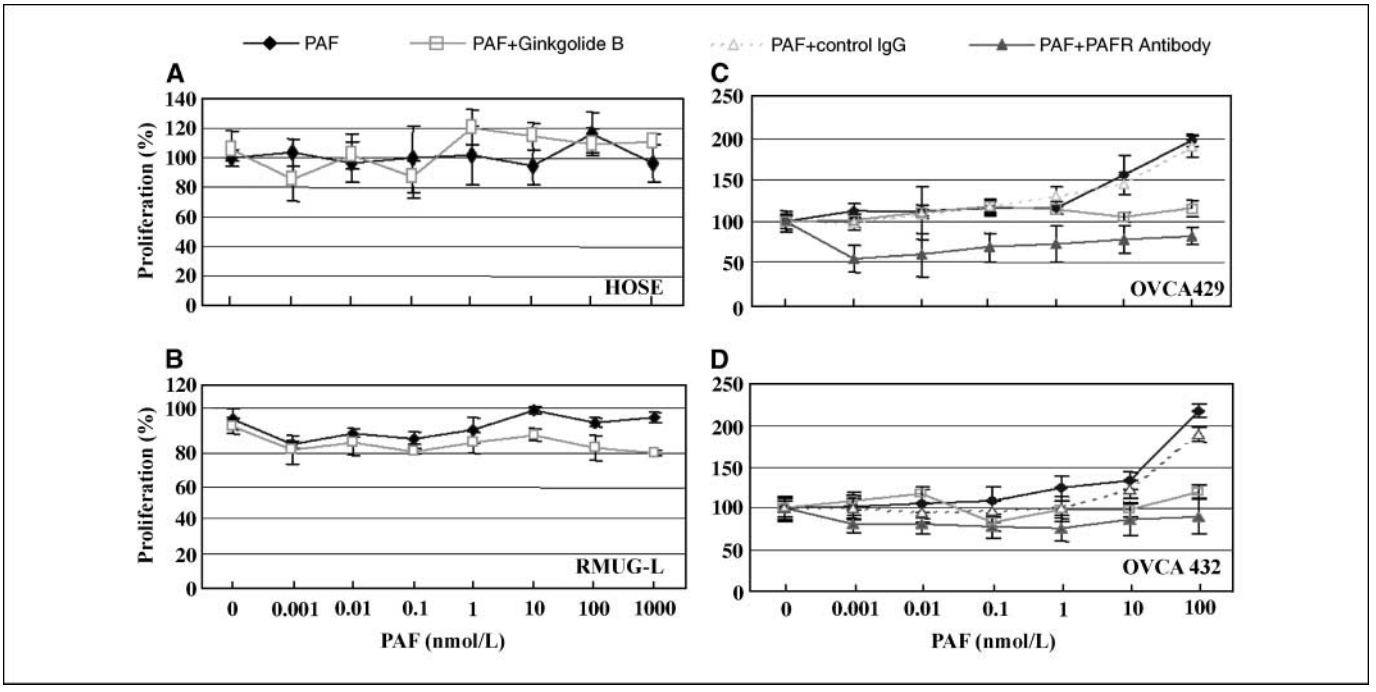

Figure 3. Ovarian cancer cell proliferation response to PAF treatment is PAFR-dependent. *A,* normal HOSE cells (without PAFR expression) showed no response with different concentrations of PAF treatment. Treatment of PAF with ginkgolide B showed no response in HOSE cell proliferation. *B,* mucinous type ovarian cancer cells RMUG-L (negative PAFR expression) showed no response to PAF treatment in cell proliferation and little effect on cell proliferation when treated together with 100 μmol/L of ginkgolide B. *C* and *D,* ovarian cancer cell lines OVCA429 and OVCA432 showed a strong and dose-dependent response to PAF treatment and significant increases in cell proliferation. Both PAFR antagonist, ginkgolide B (□) and specific antibody against PAFR (▲) have significantly blocked the PAF-induced cell proliferation, compared with treatment of PAF alone (♦) or PAF with IgG control (△; P < 0.001).

natural antagonist ginkgolide B were exogenously administered to the cultured cells under serum-free conditions. After 72 hours of incubation with different concentrations of PAF, both PAFR-negative normal HOSE and mucinous RMUG-L cells showed no significant response (Fig. 3*A* and *B*). Cell proliferation was significantly increased by PAF treatment (10 nmol/L) in OVCA429 and OVCA432 cells (Fig. 3*C* and *D*). In addition, PAF-induced cell proliferation in these cancer cells was almost completely inhibited by the administration of 100 μmol/L of ginkgolide B and a 1:50 dilution of PAFR antibody, compared with the treatment with PAF alone, or PAF plus IgG control.

PAFR gene knockdown and cell proliferation. To confirm that up-regulated PAFR significantly contributes to cancer cell proliferation, we conducted a functional analysis by reducing PAFR expression via siRNA interference in OVCA429 cells. Three specific siRNA probes significantly reduced PAFR gene expression by >90% compared with the negative control probe (Fig. 4*A*). Using immune blot analysis, we found that the siRNA probe–treated cells significantly decreased PAFR protein expression (Fig. 4*B*). Furthermore, we also found that transient PAFR gene-knockdown significantly decreased cell proliferation up to 60% ($P < 0.001$), compared to the cancer cells treated with the negative siRNA probe (Fig. 4*C*).

PAF-PAFR activated protein phosphorylation pattern in ovarian cancer cells. To further investigate the possible molecular mechanisms associated with the regulatory functions of PAF-PAFR in ovarian cancer, we examined a set of phosphorylation signals of the cancer-associated protein targets with their site-specific phospho-antibodies. OVCA429 cells were treated with PAFR agonist PAF alone or with PAF plus the antagonist ginkgolide B, respectively, at different time points. Site-specific phosphorylation intensity of eight protein targets simultaneously increased after 100 nmol/L of PAF treatment compared with the controls, and reached the plateau after 24 hours of treatment (Fig. 5). At 4 hours PAF treatment, tyrosine phosphorylation of protein targets (EGFR, FAK, and Src) were significantly increased by 2-fold, and by 1.8-fold at 6 hours for EGFR, FAK, Src, paxillin, and AKT. Furthermore, it seemed that only EGFR, Src, FAK, and paxillin showed the maximum blockage or inhibition of the phosphorylation by ginkgolide B treatment at 4 and 6 hours (Fig. 5*A*). Coordinated phosphorylation of EGFR, Src, FAK, and paxillin by PAF was further validated by Western blot analysis on both OVCA429 and OVCA432 cells (Fig. 5*B* and *C*). Phosphorylation of these proteins, however, was not observed in RMUG-L cancer cells, as expected, based on its negative PAFR expression (Fig. 5*D*).

PAF-induced ovarian cancer cell proliferation and invasion are mediated by PAFR and tyrosine phosphorylation EGFR, Src, FAK, and paxillin. After 6 hours of treatment with PAF (100 nmol/L) on OVCA429 cells, the phospho-signals of EGFR (pY^{1068}), Src (pY^{418}), FAK (pY^{397}), and paxillin (pY^{118}) were increased in Western blot and consistent with the data in phospho-antibody array (Fig. 5*A* and *B*). However, when cells were treated with ginkgolide B plus PAF, EGFR was less affected. The phosphorylation signals of Src, FAK, and paxillin were decreased and returned to the constitutive levels (Fig. 6*A*). The specific Src inhibitor PP2 showed the expected strong inhibition on Src and as well as on FAK, but had less effect on EGFR and paxillin. The

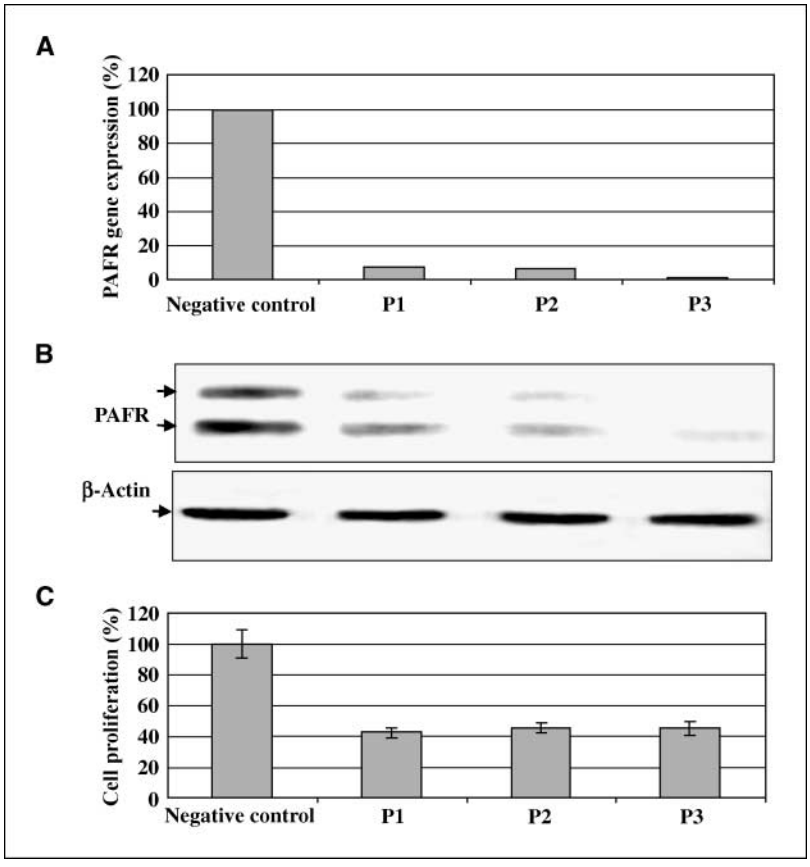

Figure 4. siRNA induced PAFR gene knockdown and decreased cell proliferation in OVCA429 ovarian cancer cells. *A,* OVCA429 cells were treated with three siRNA probes and showed near-complete deletion of PAFR gene expression compared with negative control probes. *B,* after siRNA induced PAFR gene knockdown, PAFR protein expression was depleted in the treated OVCA429 cancer cells, compared with negative controls. *C,* OVCA429 cells with siRNA treatment showed significant decreases in cell proliferation by up to 60% (*, $P < 0.0001$).

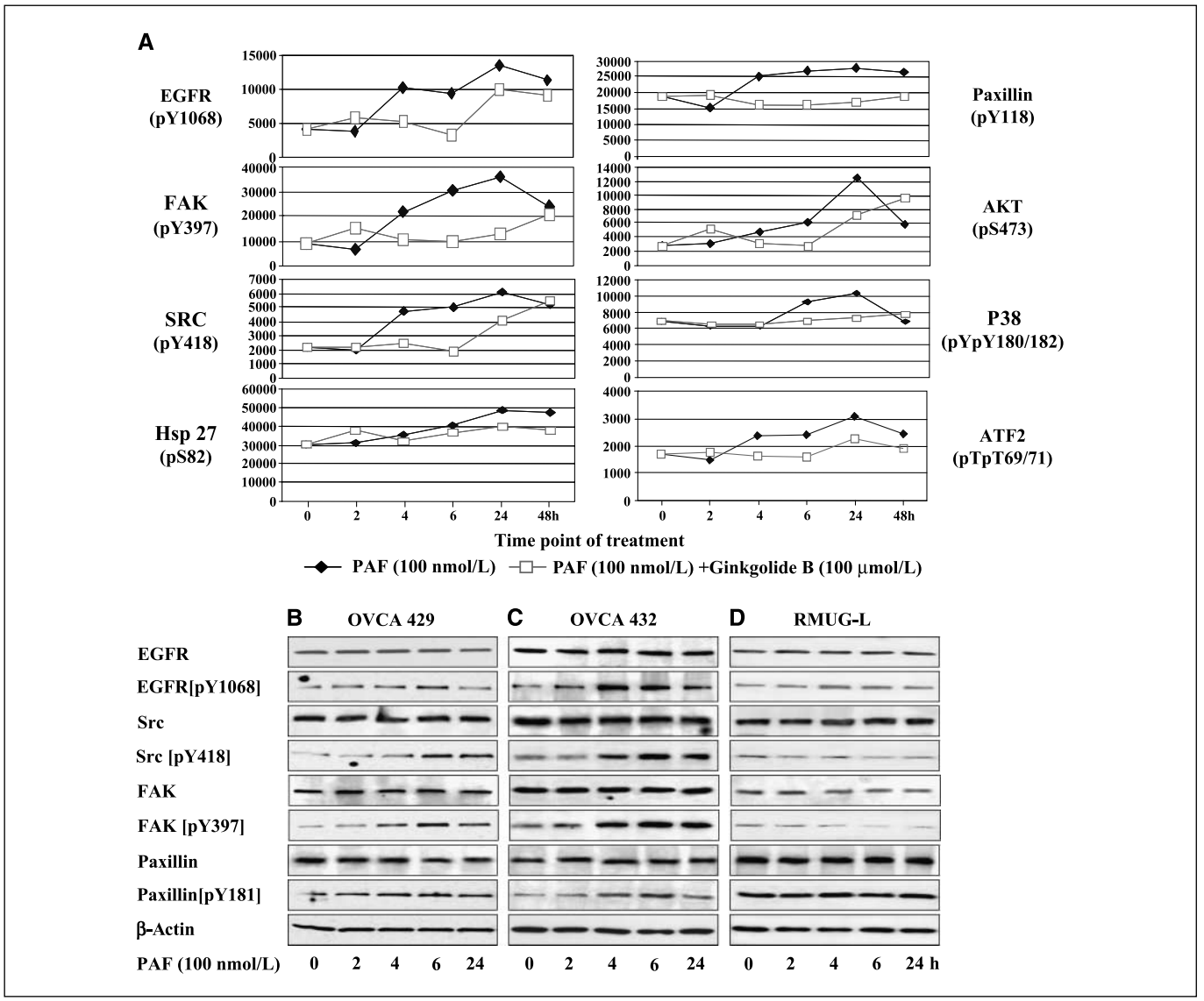

Figure 5. PAF-PAFR pathways associated with multiple protein targets and signal pathways. *A,* profiling and quantitative analysis of eight phospho-proteins using multiplex of Mercator phosphor-array (BioSource, Invitrogen, Inc.). OVCA429 cells were cultured in the serum-free medium. At 50% to 70% confluence, cells were treated with PAF and ginkgolide B dissolved in DMSO. Cell lysates of the untreated (0 h), treated with PAF (100 nmol/L; ♦), alone or a combination of PAF (100 nmol/L) and ginkgolide B (100 μmol/L; □) at different time points were subjected to Mercator phosphor-array analysis. All measurements were performed in triplicate and showed high signal uniformity and reproducibility (SEs were not shown). Western blots revealed the protein phosphorylation pattern of EGFR, Src, FAK, and paxillin after treatment with PAF (100 nmol/L) in OVCA429 (*B*), OCVA432 (*C*), and RMUG-L (*D*) cells, respectively, at different time points. Equal loading of protein was calibrated with β-actin. EGFR protein was not detectable in RMUG-L cells using the EGFR (pY^{1068}) antibody, and a fragment of phospho-EGFR (64 kDa; *D*).

nonspecific inhibitor A25 showed medium inhibition on all these targets, except for EGFR, in which a strong inhibitory effect was observed. Combined treatment of PP2 and A25 showed a similar inhibition pattern as PP2 alone. After 24 hours of treatment with PAF, the downstream protein targets PI3K and cyclin D1 associated with cell proliferation, and MMP2/MMP9 associated with cancer cell invasion, were significantly increased. The induced protein expression was decreased upon treatment with PAF, ginkgolide B, and the inhibitors (Fig. 6*A*). To define how PAF-PAFR and tyrosine phosphorylation of EGFR and Src are involved in ovarian cancer proliferation, we measured the inhibitory effects of ginkgolide B, EGFR, and Src inhibitors (erlotinib and PP2, respectively) on OVCA429 and OVCA432 cell proliferation. After 72 hours of treatment with PAF (100 nmol/L), the cell proliferation rate was increased up to 2-fold in both cell lines. The specific PAFR antagonist ginkgolide B (100 μmol/L) and the PAFR polyclonal antibody showed significant and similar intensities of inhibition, compared with the IgG controls (Fig. 6*B* and *C*). Specific Src inhibitor PP2, either used alone or combined with A25, was the strongest inhibitor in cell proliferation compared with the nonspecific inhibitor A25. Interestingly, the PI3K inhibitor LY294002 showed a similar effect on cell proliferation compared with PP2. The EGFR inhibitor (erlotinib) was less potent, but still significant in cell proliferation inhibition compared with the nonspecific inhibitor A25. Similarly, PAF-induced ovarian cancer cell invasion was also investigated in OVCA429 and OVCA432 cell lines. We showed that blocking PAFR by using ginkgolide B and specific antibody significantly ($P < 0.001$) reduced cancer cell

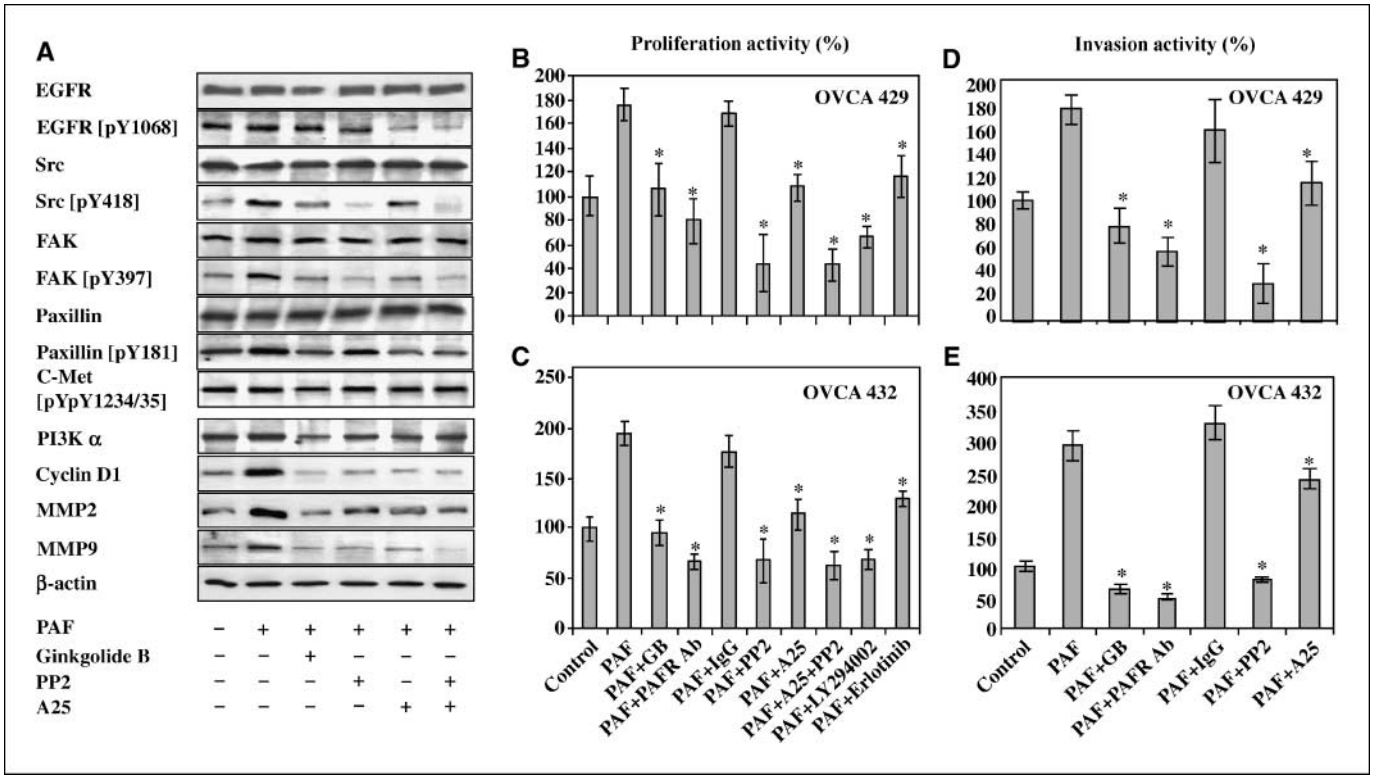

Figure 6. PAF-PAFR and Src pathways in ovarian cancer cell proliferation and invasion. *A,* after 6 h of treatment with PAF (100 nmol/L) alone (*lane 2*) and combination of PAF with ginkgolide B (100 μmol/L, *lane 3*), tyrosine-Src kinase inhibitors PP2 (10 μmol/L, *lane 4*) and A25 (10 μmol/L, *lane 5*), and combined PP2+A25, protein phosphorylation pattern of EGFR, Src, FAK, and paxillin of OVCA429 cells was revealed by using the same set of specific antibodies in Fig. 5. Phosphorylation of c-met protein not related to PAF-PAFR was used as nonspecific control. After 24 h of treatment, OVCA429 cells were harvested for protein expression analysis of PI3K, cyclin D1, MMP2, and MMP9 by Western blots. *B* and *C,* PAF induced ovarian cancer cell proliferation in OVCA429 and OVCA432 cells. After 72 h of treatment with ginkgolide B, PAFR-specific antibody, inhibitors of PP2, A25, PP2+A25, LY294002 (10 μmol/L), and erlotinib (5 μmol/L) inhibited PAF-induced cell proliferation in both cancer cell lines ($P < 0.001$). *D* and *E,* PAF-activated ovarian cancer cell invasion in OVCA429 and OVCA432 cells were significantly ($P < 0.001$) and completely blocked by ginkgolide B, PAFR antibody, and PP2 treatment within 36 h. *Columns,* means of cell proliferation and invasion were derived from at least eight repeats for proliferation, five repeats for invasion from two experiments; *bars,* SD. A polyclonal antibody against PAFR (0.5 mg/mL) was diluted 1:50 in serum-free medium and calibrated with an equal volume of nonspecific pure IgG as negative control.

invasion, which was induced by PAF treatment (Fig. 6*D* and *E*). Not surprisingly, Src inhibitor PP2 has shown a stronger inhibitory effect on OVCA429 cell invasion compared with the nonspecific tyrosine kinase inhibitor A25.

Discussion

PAF is a well-known potent phospholipid mediator involved in diverse physiologic regulations such as cell proliferation, invasion, antiapoptosis, differentiation, and oncogenic transformation (17, 18). PAF is involved in the metastatic spread of melanoma (34) and functions through MMP and cyclic AMP-response element–binding protein (19). I.p. injection of PAF promoted lung cancer metastasis (35). Inactivation of PAF by overexpression of PAF acetylhydrolase strongly inhibited the tumor growth and vascularization of B16F10 murine melanomas and Kaposi sarcomas (36). However, the regulatory functions of PAF receptor and its associated signaling pathways have not been characterized in human cancer. Here, we showed that overexpression of PAFR gene (10-fold to 10,000-fold) was found in 8 of 11 (73%) nonmucinous types of ovarian cancer cell lines and in 57 of 76 (75%) nonmucinous types of ovarian tissue specimens (Fig. 1). We also found that PAFR protein was overexpressed in ovarian cancer cell lines and patients with cancer, but was varied across different histologic types (Fig. 2). Overexpression of PAFR was often found in nonmucinous types of ovarian cancer cells. It is not clear why the mucinous ovarian tumor expressed significantly lower levels of PAFR. Surrounding carbohydrates may significantly block the active biological factors such as PAF and tumor necrosis factor-α from entering the mucinous tumor cells to stimulate PAFR gene expression (37, 38), which only partially explains the decreased level of PAFR expression in patients with mucinous ovarian tumor.

Both PAF and PAFR significantly promoted cancer cell proliferation and invasion (39, 40). Our data showed that only the PAFR-positive cells respond to PAF and stimulate cancer cell growth and invasion (Figs. 3 and 6), whereas no effect was found in the PAFR-negative cells such as immortalized HOSE cells, mucinous cancer cells, and PAFR-knockdown cells (Figs. 3 and 4). This suggests that PAF-induced ovarian cancer cell proliferation is dependent on PAFR expression. Yet, it is still unclear how PAF interacts with its receptor PAFR and stimulates the biological signal networking during the process of cancer transformation and progression. Here, we explored multiple signaling targets using the fluorescent phospho-array of 8-Plex Mercator technology to simultaneously quantify EGFR (pY^{1068}), p38 ($pTpY^{180/182}$), Akt/PKB (pS^{473}), FAK (pY^{397}), Src (pY^{418}), paxillin (pY^{118}), HSP27 (pS^{82}), and ATF2 ($pTpT^{69/71}$) as the most common phosphorylation of protein targets associated with cancer. Interestingly, all eight molecular targets were activated by PAF treatment and subsequently inactivated by ginkgolide B treatment (Fig. 5*A*). A previous

study suggested that phospholipid-mediated protein phosphorylation cascades are often important early responses to mitogenic induction (41). For example, PAFR activated MAPK and induced epidermal cell proliferation via EGFR (25), and PAF induced the activation of tyrosine phosphorylation of FAK and paxillin in human endothelial cells (24). Here, we provide additional evidence that PAF simultaneously induced multiple protein phosphorylation including EGFR, Src, FAK, and paxillin, and that the activation is dependent on PAFR gene expression in ovarian cancer cells.

PAF-PAFR–mediated stimulation of downstream phosphorylation of multiple proteins was reported in other noncancerous types of cells such as neutrophils (42) and eosinophils (43), and involved many types of protein kinases including MAPK, protein kinase C, PI3K, protein tyrosine kinase, and G protein receptor kinase (21). However, it is still not clear how the downstream targets and the signal cascades are associated with PAF-PAFR stimulation in cancer cells. In this study, we found that specific Src inhibitor PP2 showed the strongest inhibition on protein phosphorylation, cell proliferation, and invasion among the tested inhibitors (Fig. 6*B* and *C*), suggesting that Src is a key downstream target of PAFR in ovarian cancer. The similar inhibition intensity on cell proliferation induced by PI3K-α inhibitor (LY294002) and Src inhibitor (PP2) in OVCA432 and OVCA429 may suggest that Src is the upstream target of PI3K in ovarian cancer, as shown in many other cancers (44). Ginkgolide B blocked PAF-PAFR–induced EGFR phosphorylation (Fig. 5*A*) and EGFR inhibitor erlotinib showed significant inhibition on cell proliferation, but was less potent than Src inhibitor PP2 in OVCA429 and OVCA432. This would suggest that Src is the primary downstream target of PAFR (PAFR-Src), but not PAFR-EGFR, which is involved in PAF-mediated cell proliferation. Although PI3K phosphorylation was not included in the array platform and in our Western blots, we found that PI3K protein expression (α-subunit) was significantly inhibited by ginkgolide B, an antagonist of PAFR, and PI3K inhibitor had strong inhibition on cell proliferation as PP2 (Fig. 6*B* and *C*). Further studies are required to confirm the regulatory signal pathways of PAFR-Src and PI3K in PAF-mediated ovarian cancer cell proliferation. In this study, we measured the protein expression of PI3K and cyclin D1 as markers for cell proliferation and MMP2/MMP9 for call invasion to confirm these cellular functions were induced by PAF and reversibly inhibited by PAFR antagonist ginkgolide B, PAFR antibody, and Src inhibitor PP2. In addition, the specific Src inhibitor PP2 strongly and almost equally inhibited the phosphorylation of both Src and FAK, which might seem as evidence of activation of protein-protein interaction between these two protein kinases in ovarian cancer, which was often found in many other cancers (45).

Our study showed direct evidence that PAF-PAFR is commonly activated in nonmucinous ovarian cancer cells. The phospholipid mediator PAF can activate PAFR and initiate multiple downstream signal pathways, specifically through Src/FAK and the downstream targets such as PI3K, in cancer cell proliferation and MMP2/MMP9 in cancer invasion. We believe that further studies are warranted for the understanding of the precise mechanisms and the downstream signal networking pathways regulated by PAF-PAFR, which might include Src, FAK, EGFR, paxillin, PI3K/AKT, and MAPK pathways during the ovarian cancer progression.

Disclosure of Potential Conflicts of Interest

No potential conflicts of interest were disclosed.

Acknowledgments

Received 10/5/2007; revised 4/22/2008; accepted 4/22/2008.

Grant support: National Cancer Institute R21 (CA111949-01), Dana-Farber Starr Foundation, ovarian cancer case-control study R01 (CA54419-13), and ovarian cancer Specialized Programs of Research Excellence (1P50-CA105009-01).

The costs of publication of this article were defrayed in part by the payment of page charges. This article must therefore be hereby marked *advertisement* in accordance with 18 U.S.C. Section 1734 solely to indicate this fact.

We thank Dr. Ross S. Berkowitz for his encouragement and Dr. Michael J. Birrer for providing us the ovarian cancer tissue arrays to support this project.

References

1. Zhu T, Gobeil F, Vazquez-Tello A, et al. Intracrine signaling through lipid mediators and their cognate nuclear G-protein-coupled receptors: a paradigm based on PGE2, PAF, LPA1 receptors. Can J Physiol Pharmacol 2006;84:377–91.
2. Stafforini DM, McIntyre TM, Zimmerman GA, Prescott SM. Platelet-activating factor, a pleiotrophic mediator of physiological and pathological processes. Crit Rev Clin Lab Sci 2003;40:643–72.
3. Boccellino M, Camussi G, Giovane A, et al. Platelet-activating factor regulates cadherin-catenin adhesion system expression and β-catenin phosphorylation during Kaposi's sarcoma cell motility. Am J Pathol 2005;166:1515–22.
4. Hikiji H, Ishii S, Shindou H, Takato T, Shimizu T. Absence of platelet-activating factor receptor protects mice from osteoporosis following ovariectomy. J Clin Invest 2004;114:85–93.
5. Prescott SM, Zimmerman GA, Stafforini DM, McIntyre TM. Platelet-activating factor and related lipid mediators. Annu Rev Biochem 2000;69:419–45.
6. Eisinger AL, Prescott SM, Jones DA, Stafforini DM. The role of cyclooxygenase-2 and prostaglandins in colon cancer. Prostaglandins Other Lipid Mediat 2007;82:147–54.
7. Sheng H, Shao J, Washington MK, DuBois RN. Prostaglandin E2 increases growth and motility of colorectal carcinoma cells. J Biol Chem 2001;276:18075–81.
8. Tsujii M, DuBois RN. Alterations in cellular adhesion and apoptosis in epithelial cells overexpressing prostaglandin endoperoxide synthase 2. Cell 1995;83:493–501.
9. Mills GB, Moolenaar WH. The emerging role of lysophosphatidic acid in cancer. Nat Rev Cancer 2003;3:582–91.
10. Symowicz J, Adley BP, Woo MM, et al. Cyclooxygenase-2 functions as a downstream mediator of lysophosphatidic acid to promote aggressive behavior in ovarian carcinoma cells. Cancer Res 2005;65:2234–42.
11. Ulrich CM, Bigler J, Potter JD. Non-steroidal anti-inflammatory drugs for cancer prevention: promise, perils and pharmacogenetics. Nat Rev Cancer 2006;6:130–40.
12. Boucharaba A, Serre CM, Gres S, et al. Platelet-derived lysophosphatidic acid supports the progression of osteolytic bone metastases in breast cancer. J Clin Invest 2004;114:1714–25.
13. Walterscheid JP, Ullrich SE, Nghiem DX. Platelet-activating factor, a molecular sensor for cellular damage, activates systemic immune suppression. J Exp Med 2002;195:171–9.
14. Albini A, Sporn MB. The tumour microenvironment as a target for chemoprevention. Nat Rev Cancer 2007;7:139–47.
15. Liebmann C. G protein-coupled receptors and their signaling pathways: classical therapeutical targets susceptible to novel therapeutic concepts. Curr Pharm Des 2004;10:1937–58.
16. Dorsam RT, Gutkind JS. G-protein-coupled receptors and cancer. Nat Rev Cancer 2007;7:79–94.
17. Kume K, Shimizu T. Platelet-activating factor (PAF) induces growth stimulation, inhibition, and suppression of oncogenic transformation in NRK cells overexpressing the PAF receptor. J Biol Chem 1997;272:22898–904.
18. Heon Seo K, Ko HM, Kim HA, et al. Platelet-activating factor induces up-regulation of antiapoptotic factors in a melanoma cell line through nuclear factor-κB activation. Cancer Res 2006;66:4681–6.
19. Melnikova VO, Mourad-Zeidan AA, Lev DC, Bar-Eli M. Platelet-activating factor mediates MMP-2 expression and activation via phosphorylation of cAMP-response element-binding protein and contributes to melanoma metastasis. J Biol Chem 2006;281:2911–22.
20. Denizot Y, Descottes B, Truffinet V, et al. Platelet-activating factor and liver metastasis of colorectal cancer. Int J Cancer 2005;113:503–5.
21. Ishii S, Shimizu T. Platelet-activating factor (PAF) receptor and genetically engineered PAF receptor mutant mice. Prog Lipid Res 2000;39:41–82.
22. Lukashova V, Asselin C, Krolewski JJ, Rola-Pleszczynski M, Stankova J. G-protein-independent activation of Tyk2 by the platelet-activating factor receptor. J Biol Chem 2001;276:24113–21.
23. Deo DD, Axelrad TW, Robert EG, et al. Phosphorylation of STAT-3 in response to basic fibroblast growth factor occurs through a mechanism involving platelet-activating factor, JAK-2, and Src in human umbilical vein endothelial cells. Evidence for a dual kinase mechanism. J Biol Chem 2002;277:21237–45.
24. Soldi R, Sanavio F, Aglietta M, et al. Platelet-activating factor (PAF) induces the early tyrosine

phosphorylation of focal adhesion kinase (p125FAK) in human endothelial cells. Oncogene 1996;13:515–25.
25. Marques SA, Dy LC, Southall MD, et al. The platelet-activating factor receptor activates the extracellular signal-regulated kinase mitogen-activated protein kinase and induces proliferation of epidermal cells through an epidermal growth factor-receptor-dependent pathway. J Pharmacol Exp Ther 2002;300:1026–35.
26. Fang X, Schummer M, Mao M, et al. Lysophosphatidic acid is a bioactive mediator in ovarian cancer. Biochim Biophys Acta 2002;1582:257–64.
27. Gupta GP, Massague J. Platelets and metastasis revisited: a novel fatty link. J Clin Invest 2004;114:1691–3.
28. Ye B, Aponte M, Dai Y, et al. Ginkgo biloba and ovarian cancer prevention: Epidemiological and biological evidence. Cancer Lett 2007;251:43–52.
29. Tsao SW, Mok SC, Fey EG, et al. Characterization of human ovarian surface epithelial cells immortalized by human papilloma viral oncogenes (HPV-E6E7 ORFs). Exp Cell Res 1995;218:499–507.
30. Mosmann T. Rapid colorimetric assay for cellular growth and survival: application to proliferation and cytotoxicity assays. J Immunol Methods 1983;65:55–63.
31. Tsuda H, Ito YM, Ohashi Y, et al. Identification of overexpression and amplification of ABCF2 in clear cell ovarian adenocarcinomas by cDNA microarray analyses. Clin Cancer Res 2005;11:6880–8.
32. Livak KJ, Schmittgen TD. Analysis of relative gene expression data using real-time quantitative PCR and the 2(-ΔΔC(T)) method. Methods 2001;25:402–8.
33. Garcia Rodriguez C, Cundell DR, Tuomanen EI, et al. The role of N-glycosylation for functional expression of the human platelet-activating factor receptor. Glycosylation is required for efficient membrane trafficking. J Biol Chem 1995;270:25178–84.
34. Melnikova V, Bar-Eli M. Inflammation and melanoma growth and metastasis: the role of platelet-activating factor (PAF) and its receptor. Cancer Metastasis Rev 2007;26:359–71.
35. Im SY, Ko HM, Kim JW, et al. Augmentation of tumor metastasis by platelet-activating factor. Cancer Res 1996;56:2662–5.
36. Biancone L, Cantaluppi V, Del Sorbo L, et al. Platelet-activating factor inactivation by local expression of platelet-activating factor acetyl-hydrolase modifies tumor vascularization and growth. Clin Cancer Res 2003;9:4214–20.
37. Mutoh H, Ishii S, Izumi T, Kato S, Shimizu T. Platelet-activating factor (PAF) positively auto-regulates the expression of human PAF receptor transcript 1 (leukocyte-type) through NF-κB. Biochem Biophys Res Commun 1994;205:1137–42.
38. Dagenais P, Thivierge M, Parent JL, Stankova J, Rola-Pleszczynski M. Augmented expression of platelet-activating factor receptor gene by TNF-α through transcriptional activation in human monocytes. J Leukoc Biol 1997;61:106–12.
39. Bussolati B, Biancone L, Cassoni P, et al. PAF produced by human breast cancer cells promotes migration and proliferation of tumor cells and neo-angiogenesis. Am J Pathol 2000;157:1713–25.
40. Cellai C, Laurenzana A, Vannucchi AM, et al. Growth inhibition and differentiation of human breast cancer cells by the PAFR antagonist WEB-2086. Br J Cancer 2006;94:1637–42.
41. Rozengurt E. Mitogenic signaling pathways induced by G protein-coupled receptors. J Cell Physiol 2007;213:589–602.
42. Mollapour E, Linch DC Roberts PJ. Activation and priming of neutrophil nicotinamide adenine dinucleotide phosphate oxidase and phospholipase A(2) are dissociated by inhibitors of the kinases p42(ERK2) and p38(SAPK) and by methyl arachidonyl fluorophosphonate, the dual inhibitor of cytosolic and calcium-independent phospholipase A(2). Blood 2001;97:2469–77.
43. Sotsios Y, Ward SG. Phosphoinositide 3-kinase: a key biochemical signal for cell migration in response to chemokines. Immunol Rev 2000;177:217–35.
44. Tanaka Y, Kobayashi H, Suzuki M, Kanayama N, Terao T. Transforming growth factor-β1-dependent urokinase up-regulation and promotion of invasion are involved in Src-MAPK-dependent signaling in human ovarian cancer cells. J Biol Chem 2004;279:8567–76.
45. McLean GW, Carragher NO, Avizienyte E, et al. The role of focal-adhesion kinase in cancer—a new therapeutic opportunity. Nat Rev Cancer 2005;5:505–15.